
BlockDialect: Block-wise Fine-grained Mixed Format for Energy-Efficient LLM Inference

Wonsuk Jang¹ Thierry Tambe¹

Abstract

Large Language Models (LLMs) have achieved remarkable success, but their increasing size poses significant challenges in memory usage and computational costs. Quantizing both weights and activations can address these issues, with fine-grained block-wise quantization emerging as a promising hardware-supported solution to mitigate outliers. However, existing methods struggle to capture nuanced block data distributions. To address this, we propose BlockDialect, a block-wise fine-grained mixed format technique that assigns a per-block optimal number format from formatbook for better data representation. Additionally, we introduce DialectFP4, a formatbook of FP4 variants (akin to *dialects*) that adapt to diverse data distributions. To leverage this efficiently, we propose a two-stage approach for online DialectFP4 activation quantization. Importantly, DialectFP4 ensures hardware efficiency by selecting representable values as scaled integers compatible with low-precision integer arithmetic. BlockDialect achieves 11.83% (7.56%) accuracy gain on the LLaMA3-8B (LLaMA2-7B) model compared to MXFP4 format with lower bit usage per data, while being only 5.46% (2.65%) below full precision even when quantizing full-path matrix multiplication. Focusing on *how to represent* over *how to scale*, our work presents a promising path for energy-efficient LLM inference.

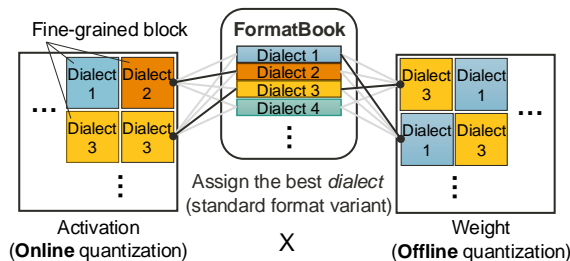


Figure 1. Overview of BlockDialect technique workflow.

caused by limited memory capacity and high data movement between memory and accelerators (Frantar et al., 2022; Alizadeh et al., 2023; Gholami et al., 2024). Moreover, the increase in model size leads to substantially more multiply-accumulate (MAC) operations, thereby escalating computational costs (Xiao et al., 2023). To tackle these issues, quantization has emerged as a crucial technique (Gholami et al., 2022). By lowering the precision of numerical representations, quantization effectively reduces memory needs and data movement overhead (Kim et al., 2023). Additionally, leveraging low-precision operation results in improvements in inference speed, area, and energy efficiency (Xiao et al., 2023; Cao et al., 2024; Rouhani et al., 2023a).

A key challenge in LLM quantization lies in handling outliers - elements with much larger magnitudes compared to the rest (Dettmers et al., 2022). Quantization typically involves scaling elements using a scaling factor determined by the maximum magnitude. However, outliers can skew the scaling factor, leading to diminished representation capacity for the majority of the elements (Liu et al., 2023a). To counter this issue, block-wise quantization has been adopted as a common solution (Frantar et al., 2022; Dettmers et al., 2023; Lin et al., 2024; Sheng et al., 2023). By dividing the tensor into smaller blocks and quantizing each block separately, this method effectively mitigates the influence of outliers within localized areas.

While smaller blocks encapsulate outliers better, they introduce overhead in managing high-precision scaling factors (Rouhani et al., 2023a). Recent advancements have focused on using hardware support for fine-grained block-wise quantization at the sub-token/channel level (e.g., block

1. Introduction

Large Language Models (LLMs) have achieved remarkable success in various tasks (Zhang et al., 2022), prompting researchers to create even larger models to enhance performance (Chowdhery et al., 2023; Dubey et al., 2024). However, this exponential growth in model sizes presents significant challenges, particularly a critical memory bottleneck

¹Department of Electrical Engineering, Stanford University. Correspondence to: Wonsuk Jang <wsjang@stanford.edu>, Thierry Tambe <ttambe@stanford.edu>.

size 32) (Rouhani et al., 2023a; Dai et al., 2021; Rouhani et al., 2023b). In line with this progress, Open Compute Project, backed by leading tech companies, has established the Microscaling (MX) format specification¹. This format enhances performance and hardware efficiency via fine-grained blocks and power-of-two scaling factors, and has been adopted by AI accelerators like NVIDIA’s Blackwell².

In addition to advancements in block-wise quantization, research has also pushed the boundaries of extremely low-bit quantization, reaching even 2-bit precision (Egiazarian et al., 2024; Chee et al., 2024). However, most approaches focus on weight-only quantization due to challenges in quantizing activations which are: (1) the need for real-time quantization, (2) a wider dynamic range, and (3) channel-wise variances that misalign with matrix multiplication dimensions (Xiao et al., 2023). As a result, high-precision activations require dequantizing weights and performing arithmetic operations at high precision (Dotzel et al., 2024), reducing potential gains in energy efficiency and inference throughput. Furthermore, as sequence lengths increase in modern LLMs, the quadratic growth in computational demands exacerbates these inefficiencies (Keles et al., 2023; Shyam et al., 2024). Thus, addressing activation quantization is critical for realizing compute- and energy-efficient LLM inference.

Our work stems from the insight: *“If a group of numbers deserves its own scaling factor, why not its own number format?”* Existing research primarily focuses on *“how to scale”* activations to make them quantization-friendly, often by migrating quantization difficulty to weights (Xiao et al., 2023) or utilizing Hadamard matrices to reduce outliers (Ashkboos et al., 2024). In contrast, we take a novel perspective by exploring *“how to represent”* each block, leveraging hardware-supported fine-grained block-wise quantization. We propose BlockDialect, which enables 4-bit weight and activation post-training quantization with each block assigned an optimal number format from a formatbook.

Additionally, we present DialectFP4: a formatbook of FP4 variants tailored to capture diverse block-wise data distributions. To efficiently leverage this, we propose a two-stage approach for optimal format selection, followed by logical operations for online DialectFP4 activation quantization. The effectiveness of our on-the-fly activation quantization scheme is affirmed by delivering zero-shot performance on par with an exact mean squared error (MSE)-based approach. Importantly, DialectFP4 is designed for hardware-friendly operations, ensuring compatibility with integer arithmetic by selecting representable values as scaled integers. This property enables our MAC unit to achieve the same level of

area and energy efficiency as FP4 MAC units. To maximize energy efficiency, we further extend our approach to *full-path* matrix multiplications, including activation-activation multiplications, while ensuring robust performance.

BlockDialect demonstrates significant improvements over the MXFP4 format, achieving 11.83% (7.56%) higher zero-shot accuracy performance with lower bit usage per data, while showing only 5.46% (2.65%) lower accuracy than full precision on the LLaMA3-8B (LLaMA2-7B) for full-path quantization. When quantizing only linear layers, BlockDialect achieves a marginal 1.77% (1.20%) accuracy drop compared to full precision. Our contributions can be summarized as follows:

- We introduce BlockDialect, a novel block-wise fine-grained mixed format technique that assigns an optimal number format to each block, enabling accurate representation of data distribution in LLMs.
- We propose DialectFP4, a set of FP4 E2M1 variants tailored for diverse block-level distributions while maintaining hardware efficiency.
- We achieve online DialectFP4 activation quantization through a practical two-stage approach, yielding accuracy on par with an exact MSE-based approach.
- We demonstrate that our approach outperforms existing methods across multiple LLMs while leveraging low-precision, energy-efficient MAC units.

2. Related Work

Quantization-aware training (QAT) (Liu et al., 2023b) and post-training quantization (PTQ) (Nagel et al., 2020; Frantar et al., 2022) are two primary DNN quantization approaches, with PTQ emerging as a more practical solution for large models. However, maintaining model accuracy remains challenging for PTQ, particularly at extremely low precision. Research has focused on addressing outliers and adopting novel number formats to minimize quantization error.

2.1. Block-wise Quantization

Block-wise (or group-wise) quantization is a widely adopted technique that assigns scaling factors on a per-block basis, effectively constraining the impact of outliers within each block. To determine these scaling factors, two methods can be employed: software-supported and hardware-supported.

Software-supported methods (Frantar et al., 2022; Dettmers et al., 2023; Lin et al., 2024; Sheng et al., 2023) typically rely on high-precision scaling factors, enhancing accuracy but often require larger block sizes due to the overhead of storing and applying scaling factors. In contrast, hardware-supported techniques allow finer-grained blocks by using hardware-friendly scaling factors, such as power-of-two

¹<https://www.opencompute.org/documents/ocp-microscaling-formats-mx-v1-0-spec-final-pdf>

²<https://www.nvidia.com/en-us/data-center/tensor-cores/>

shared exponents. VS-Quant (Dai et al., 2021) and Micro-exponents (Rouhani et al., 2023a) demonstrated the effectiveness of this approach, further enhanced by multi-level scaling factors through dedicated hardware. The Open Compute Project recently introduced the microscaling (MX) format (Rouhani et al., 2023b), which uses shared exponents across low-precision formats like FP4 and FP6. Its adoption in recent accelerators² highlights ongoing industry efforts to enhance hardware support for fine-grained scaling. Building on these advancements, our work introduces a novel approach that assigns number formats on a per-fine-grained block basis, combining with per-block scaling factors to effectively reduce quantization error.

2.2. Non-Uniform Quantization

Non-uniform quantization has been extensively explored as alternatives to integer formats, aiming to better capture data distributions in LLMs. Floating-point formats have proven effective for handling wide value ranges encountered in deep learning models. FP8-Quantization (Kuzmin et al., 2022) highlights how FP8 outperforms INT8 by effectively addressing outliers through its flexible exponent representation. ZeroQuant-FP (Wu et al., 2023) demonstrates that floating-point formats strike a better balance between dynamic range and precision compared to integer formats. Also, the adoption of FP8 and FP4 by NVIDIA GPUs demonstrates their practicality.

To further improve the flexibility of representable values, lookup-based formats have emerged as promising alternatives. NF4 (Dettmers et al., 2024) and SF4 (Dotzel et al., 2024) leverage statistical distribution quantile functions (normal and Student’s t distribution, respectively) to better align with LLM profiles. Vector quantization extends this concept by performing vector-level matching with codebooks, with AQLM (Egiazarian et al., 2024) offering enhanced performance through multi-level codebooks and QuIP# (Tseng et al., 2024) proposing cache-efficient compressed codebook solutions. However, these methods typically rely on high-precision operations using retrieved high-precision values, incurring significant compute and energy overhead. Our work addresses these limitations by using DialectFP4, FP4 variants that capture block-level distributions and are compatible with low-precision integer arithmetic, offering superior hardware efficiency than high-precision MACs.

2.3. Activation Quantization

Activation quantization presents challenges due to the need for real-time execution, large dynamic ranges, and misalignment of inter-channel variance with matrix multiplication dimensions. Researchers have developed various approaches to address these issues: 1) LLM.int8() (Dettmers et al., 2022) and Atom (Zhao et al., 2024) employs mixed pre-

cision subgrouping, retaining outliers in high precision to minimize performance degradation. However, this approach incurs non-negligible overhead due to the use of mixed precision. 2) SmoothQuant (Xiao et al., 2023) migrates quantization difficulty from activations to weights, enabling 8-bit quantization for both weights and activations, avoiding high-precision operations. 3) Recent advancements using Hadamard matrices directly reduce outliers while maintaining computational invariance. This enables effective 4-bit weight, activation, and KV cache quantization (Ashkboos et al., 2024; Liu et al., 2024b). However, it incurs overhead from the online Hadamard transformation for 4-bit activation quantization and partially retain high-precision components (e.g., queries). 4) Mixed-format quantization, similar to our approach, selects the optimal number formats from candidates for predefined granularities. For example, LLM-FP4 (Liu et al., 2023a) adjusts number formats and exponent biases for each matrix to determine the best configuration, while MoFQ (Zhang et al., 2024) applies layer-wise format selection between floating point and integer. However, these methods lack adaptability to varying data distributions due to their relatively coarse and limited customization strategies.

Our work refines the mixed-format concept by introducing FP4 variants (*dialects*) that effectively capture diverse large magnitude distributions with only slight differences in representable values. These formats are assigned to fine-grained blocks in real-time, avoiding sample sensitivity in number format selection. To simplify the terminology and highlight the use of variants over completely distinct formats, the term *dialect* will be used from now on instead of variants or candidates of formatbook. It is worth mentioning that our work addresses the number format selection problem, making our technique complementary to existing methods, such as difficulty migration or outlier reduction through Hadamard matrices.

3. BlockDialect: Block-wise Fine-grained Mixed Format

To achieve block-wise fine-grained mixed-format quantization, we address three key questions: 1) Which *dialects* should be used? 2) How should the per-block *dialect* be selected? 3) How should online quantization and MAC operations be performed?

3.1. Which Dialects Should be Used?

Block-Level Profiling. To provide a guideline for determining dialects for the formatbook, we conducted a detailed profiling of Llama3-8B (Dubey et al., 2024), Llama2-7B (Touvron et al., 2023), and Mistral-7B (Jiang et al., 2023) models using WikiText2 (Merity et al., 2016). Our methodology involved splitting each matrix into blocks of size 32, scaling

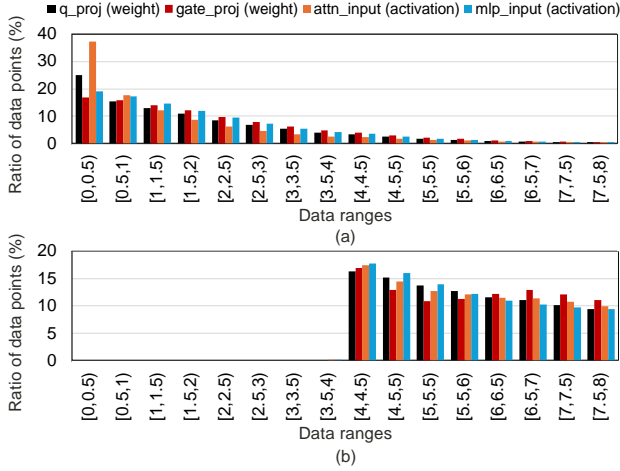


Figure 2. LLaMA3-8B block-level profiling results: (a) matrix-wise accumulated magnitude distribution, (b) block’s maximum magnitude distribution.

each block by $\lfloor \log_2(\text{block's maximum magnitude}) \rfloor - 2$, and accumulating magnitude distribution histograms for each block (Figure 2 presents the average results for layers 0, 10, 20, and 30 of the LLaMA3 model). The overall trend remains consistent across layers. The results for other models are provided in the Appendix A). Note that as we leverage hardware-supported fine-grained scaling, the scaling factor is power-of-two, which results in the power-of-two dynamic range. The subtraction of two facilitates direct comparison with FP4 E2M1, which has a dynamic range of 0 to 6.

Our matrix-wise analysis revealed that FP4 E2M1 (2 exponent bits with bias 1, 1 mantissa bit) closely aligns with the shape of the observed distribution. Specifically, the values are densely concentrated in the 0–2 range, sparser between 2–4, and highly sparse between 4–8, patterns that mirror the distribution of representable values in FP4 E2M1 (Figure 2a). Based on these findings, we selected FP4 E2M1 as our base number format for dialects.

However, upon closer examination of individual block magnitude distributions, we uncovered two important trends. First, the maximum magnitude of each block is relatively evenly distributed (Figure 2b). Second, some blocks exhibit distributions that deviate from the overall matrix-wise distribution, which shows more sparsity at the outer bound of the range. For example, certain blocks display multiple values around 7.5 but no values within the [4, 7] range. The aforementioned findings were similarly observed across different LLMs (Appendix A). These observations emphasize the importance of aligning with the specific distribution of each block, from which we derive three core principles for the development of our formatbook: 1) minimizing wasted or underestimated ranges, 2) prioritizing the representation of larger magnitudes, and 3) ensuring hardware efficiency.

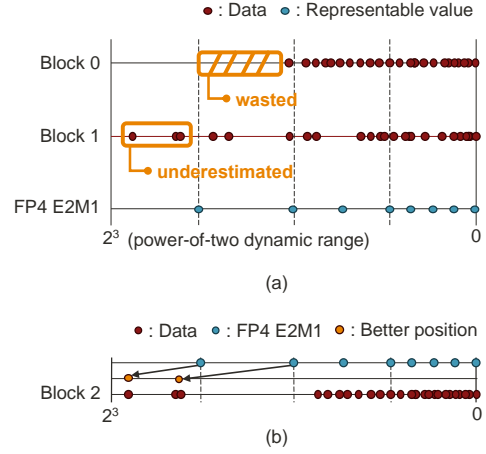


Figure 3. Core observations that inform the development of the formatbook: (a) wasted or underestimated ranges, (b) unique distributions that FP4 E2M1 fails to capture effectively.

Minimizing Wasted or Underestimated Ranges. Each block has its own dynamic range, but the use of power-of-two shared exponents results in power-of-two dynamic ranges. This mismatch leads to wasted or underestimated range problems for certain blocks. Figure 3a illustrates examples of these cases. For blocks with maximum magnitudes smaller than 6 (the maximum representable value of FP4 E2M1), the range beyond the maximum magnitude is wasted, as no data points can be mapped to the representable values within this range. For instance, if a block’s maximum magnitude is 4.5, the maximum representable value of FP4 E2M1 (which is 6) could be better utilized if the range were scaled to lie between 0 and 4.5. Conversely, for blocks containing data points larger than 6, these values cannot be represented and are thus underestimated by FP4 E2M1. This leads to our first criterion: including FP4 dialects with different maximum magnitudes.

Prioritizing the Representation of Larger Magnitudes. Large magnitudes, especially outliers, are more likely to yield higher values after multiplication, indicating their greater importance, as similarly noted by other works (Lin et al., 2024; Dettmers et al., 2022). Likewise, we assume that larger magnitudes in each block are also of relatively greater importance. Given the constraints of 4-bit representation, which allows for only 8 distinct representable magnitudes, our approach prioritizes the accurate expression of larger values over smaller ones. Our profiling shows that the matrix-wise scaled magnitude distribution becomes increasingly sparse at the outer bound, whereas each block’s scaled data distribution does not necessarily follow this pattern. Therefore, simply adjusting the exponent bias is insufficient as such methods fail to capture the nuanced distributions within specific blocks. Consequently, we establish our second criterion: generating dialects capable of representing a

Dialect 0	7.5	5.5	3	2	1.5	1	0.5	0
Dialect 1	7.5	4.5	3	2	1.5	1	0.5	0
Dialect 2	7	5.5	3	2	1.5	1	0.5	0
Dialect 3	7	4.5	3	2	1.5	1	0.5	0
Dialect 4	6.5	5	3	2	1.5	1	0.5	0
Dialect 5	6.5	4	3	2	1.5	1	0.5	0
Dialect 6	6	5	3	2	1.5	1	0.5	0
Dialect 7	6	4	3	2	1.5	1	0.5	0
Dialect 8	5.5	4.5	3	2	1.5	1	0.5	0
Dialect 9	5.5	3.5	3	2	1.5	1	0.5	0
Dialect 10	5	4.5	3	2	1.5	1	0.5	0
Dialect 11	5	3.5	3	2	1.5	1	0.5	0
Dialect 12	4.5	4	3	2	1.5	1	0.5	0
Dialect 13	4.5	3.5	3	2	1.5	1	0.5	0
Dialect 14	4	3.5	3	2	1.5	1	0.5	0
Dialect 15	4	3	2.5	2	1.5	1	0.5	0

Figure 4. 16-dialect DialectFP4 example.

diverse range of large-magnitude distributions.

Ensuring Hardware Efficiency. To achieve hardware-efficient quantization, our dialects must support low-bit MAC operations. Hence, we maintain a minimum granularity equal to that of FP4 E2M1 (0.5). This approach limits the bit width used to express each value, which proves advantageous for hardware-efficient implementation (detailed in Section 3.3). Also, our use of multiple dialects requires real-time quantization of activation matrices for each selected dialect. This process cannot rely on conventional shift and round logic due to dialect variability, necessitating distinct quantization logic for each. However, implementing separate logic for every value across all dialects would be inefficient. These considerations inform our third criterion: aligning granularity with FP4 E2M1 and preserving most FP4 values to limit possible representable values. This strategy balances representational flexibility with hardware efficiency, enabling improved quantization accuracy without compromising computational overhead.

16-Dialect DialectFP4 Example. Figure 4 illustrates 16-dialect formatbook, DialectFP4, that meets our three key requirements: ① The dialects cover all possible maximum magnitudes. ② Each pair of dialects shares the maximum magnitude while differing in one representable large magnitude value, allowing for the capture of various large magnitude distributions. ③ The unit of these dialects is 0.5, aligning with FP4 E2M1, while most of the six smallest magnitude values remain consistent with FP4 E2M1. Based on this DialectFP4, each data point is stored using 4 bits: 1-bit sign and 3-bit index corresponding the value of the selected dialect. Additionally, a 4-bit dialect identifier (for 16 dialects) is assigned to each block.

3.2. How Should the Per-Block Dialect be Selected?

While the optimal per-block dialect for preknown weights can be determined by calculating the exact mean square error (MSE) for each dialect, this approach is infeasible for activations due to their dynamic nature. Many studies rely on sample datasets to extract statistical information about activations, such as channel-wise maximum magnitudes (Xiao et al., 2023), or guide quantization loss metrics (Lin et al., 2024) (e.g., minimizing output activation errors) without real-time evaluation. These methods typically operate at a coarse granularity or focus on weight-only quantization, making them less sensitive to specific sample datasets and thus feasible for such use.

In contrast, our approach targets fine-grained activation blocks, where the choice of dialect has a direct and significant impact on quantization outcomes. This sensitivity demands a more precise and adaptive method. To address this, we adopt a sample dataset-agnostic strategy that performs on-the-fly dialect selection. To this end, we propose an efficient two-stage selection process, following a preprocessing stage, as illustrated in Figure 5.

Preprocessing Stage. In the preprocessing stage, we compute a 5-bit shared exponent (FP16 exponent bit width) based on the block’s maximum magnitude, adjusting it to ensure the expression range, $[0,8)$, fully encompasses FP4 E2M1’s range, $[0,6]$. Each element’s exponent is then adjusted by subtracting the shared exponent, enabling a compact 2-bit exponent per element. For cases where the shared exponent exceeds an element’s exponent, a compensatory mantissa shift is applied. The mantissa is then shifted by the adjusted exponent, and the lower bits are truncated to form a 5-bit representation: 3-bit integer part and 2-bit fractional part (Figure 5a). This is achievable due to our 0.5 granularity, which allows accurate rounding from the second fractional bit. To be clear, this doesn’t mean 5-bit quantization; this is an intermediate value used for optimal dialect selection and quantization process.

Two-Stage Dialect Selection Process. Comparing every dialect to find the best dialect for each block is computationally expensive and inefficient. Instead, we adopt a two-stage approach. In the first stage, we narrow down the options by selecting a pair of dialects whose largest magnitudes match the block’s maximum (Figure 5b). Recall that each pair of dialects share the maximum magnitude. The block’s maximum magnitude can be easily determined by rounding from the second fractional bit ($Block_{maxTrunc}$). This step not only streamlines the selection process but also ensures that the chosen dynamic range aligns with the block’s characteristics, avoiding wasted or underestimated ranges.

In the second stage (Figure 5c), we determine the optimal dialect from the two dialects in the chosen pair by evaluat-

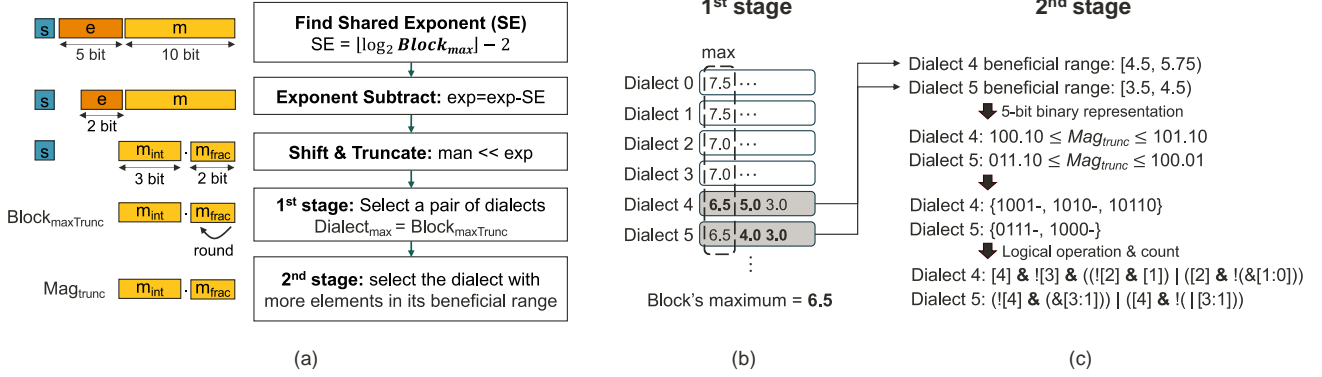


Figure 5. Per-block dialect selection process: a) overall process, b) 1st stage, c) 2nd stage.

ing which one has more block elements within its beneficial range. Since the two dialects differ by only one large magnitude value, the beneficial range is defined as the interval where incorporating this different value reduces quantization error. This range can be calculated as the midpoint between the differing value, its adjacent value, and the paired dialect’s differing value. For example, the beneficial range for dialect 4 is $[4.5, 5.75)$, where 4.5 is the midpoint between the differing values of dialect 4 and 5 $((5.0 + 4.0)/2)$, and 5.75 is the midpoint between dialect 4 and its adjacent value $((5.0 + 6.5)/2)$.

A naive approach to count elements within beneficial ranges requires four comparisons (two per each beneficial range) per element, which introduces compute and latency overhead. We can convert the range checks into efficient logical operations to optimize this process, as illustrated in Figure 5c. If we represent each beneficial range as a 5-bit binary representation and enumerate all possible cases, we can compress them into simple logical operations. In Figure 5c, we use $5'b10110$ to represent the upper limit of dialect 4’s beneficial range, excluding 5.75 ($5'b10111$). Note that $5'b10110$ encompasses all values smaller than 5.75, as we truncate after the second fractional bit. Finally, if the four most significant bits are $4'b1001$, the element falls within dialect 4’s beneficial range.

This logic can be pre-designed as we use a fixed DialectFP4. With these simple logical operations, we can efficiently count the number of elements falling within each dialect’s beneficial range in parallel. Given that we use fine-grained blocks with sizes up to 64 elements, the counting process can be further optimized using a reduction tree structure.

3.3. How Should Online Quantization and MAC Operations be Performed?

DialectFP4 uses a 0.5 granularity for representable values, expressing values from 0 to 7.5 as 4-bit unsigned integers

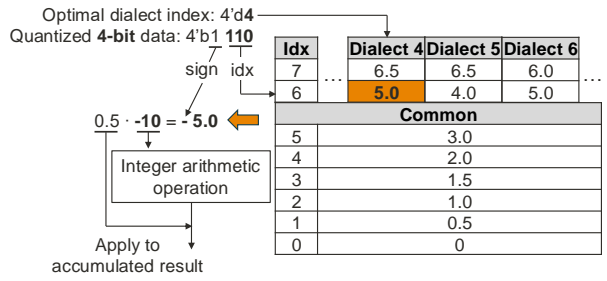


Figure 6. Overview of dequantization process.

from 0 to 15 ($0.5 * [0-15]$). Consequently, all multiplications can be efficiently performed using 4-bit unsigned integer multiplication, followed by a 2-bit right shift to account for the 0.5 factor in each number. Our quantization target is thus 4-bit (one sign bit and 3-bit index), which is then dequantized to 5 bits (previous one sign bit and 4-bit unsigned integer) before multiplication.

For weights, the optimal dialect for each block is pre-computed, with pre-quantization performed prior to inference. During inference, the 3-bit index is converted to 4-bit integers by indexing a pre-stored table of representable values (Figure 6). Most values are shared across dialects, minimizing storage requirements. Activation data, however, requires real-time quantization to the nearest representable value of the optimal dialect. For instance, consider preprocessed data (Mag_{trunc} in Figure 5) represented as $5'b10001$ in 3-bit integer and 2-bit fractional form. This corresponds to a value of 8.5 with a scaling factor 0.5. If the optimal dialect’s representable values are $0.5 * [13, 10, 6, 4, 3, 2, 1, 0]$, the value 8.5 would be quantized to 10. Note that this operation cannot be achieved using simple shift and rounding logic. In the final representation after 0.5 scaling, this maps to 5.

We can accelerate this in a hardware-efficient manner using a method similar to our optimal dialect selection process. Each representable value is associated with simple

checking logic derived from its binary form. For example, data k is quantized to 10 if it falls within $[8.0, 11.5)$, expressed as $[5'b10000, 5'b10110]$. This can be verified by $k[4] \& !k[3] \& !(k[2 : 0])$, which is true for the previous example, $5'b10001$. The quantized value is then stored in a 4-bit format including a sign bit and $3'b110$ (the index for 10 in dialect 4). The overall quantization logic can be optimized by eliminating redundant logical operations, such as the repeated use of $k[4] \& !k[3]$ across different values. Additionally, since most representable values are shared among dialects, the logic can be further simplified.

The final multiplication is performed using integer MAC operations, resulting in hardware-efficient power and area usage (detailed in Section 4.2). The MAC partial sums for each block are accumulated in FP16, followed by a 2-bit right shift for the 0.5 factor, and then requantized into a DialectFP4 4-bit data before the next matrix multiplication. Other specialized operations, such as softmax, are performed in high precision. Importantly, the optimal dialect selection, quantization, and MAC operations can be pipelined to further accelerate the overall inference speed.

4. Experiments

4.1. Experimental Setup

Models and dataset. We evaluate BlockDialect using three large language models: LLaMA-2-7B (Touvron et al., 2023), LLaMA-3-8B (Dubey et al., 2024), and Mistral-7B (Jiang et al., 2023). The evaluation includes seven zero-shot commonsense reasoning tasks: LAMBADA (Paperno et al., 2016), HellaSwag (Zellers et al., 2019), BoolQ (Clark et al., 2019), PIQA (Bisk et al., 2020), WinoGrande (Sakaguchi et al., 2021), ARC-easy, and ARC-challenge (Clark et al., 2018). For this purpose, we use the lm-eval-harness (Gao et al., 2023) framework. *0-shot* notation in this section refers to the average accuracy across seven tasks. Additionally, we report perplexity scores on WikiText2 (Merity et al., 2016) with a chunk of 2048.

Baseline. We compare BlockDialect with the MXFP4 format (Rouhani et al., 2023b), which employs hardware-supported scaling. Additionally, we compare with two recent methods using software-supported scaling: LLM-FP4 (Liu et al., 2023a), and Quarot (Ashkboos et al., 2024). Quarot reduces outliers via a rotation matrix, while LLM-FP4 uses matrix-wise mixed format. We run baselines using their open-source code³. To demonstrate BlockDialect’s applicability for full-path matrix multiplications and its potential to further enhance energy efficiency, we test two scopes: *linear* (quantization for linear layers only) and *all*

³We set (search_interval, search_round) to (60, 2) in LLM-FP4 to avoid excessive calibration time, observing negligible LLaMA-7B accuracy loss compared to the original paper.

(extends to attention block operations QK , $Attn_scoreV$). All operands are quantized along their respective multiplication dimensions, as detailed in Appendix C. We denote *Effective bitwidth* (*Eff. bit*) as the average bit width required per data, accounting for overhead from scaling factors or dialect identifiers of DialectFP4 as explained in Appendix G. In the *linear* scope, this metric focuses on linear layers; in the *all* scope, it accounts for all matrix multiplications. Block size is 32 unless otherwise specified.

Implementation. For performance evaluation, we implement the BlockDialect emulation framework extending the MX framework⁴ on top of Hugging Face Transformers with PyTorch. Specifically, we replace `nn.Linear`, `torch.matmul` with custom implementations, which include BlockDialect quantization for both operands before multiplication. All experiments were conducted on a single NVIDIA H100 GPU. For hardware comparison, we model multiply-accumulate (MAC) units for various precision levels using SystemVerilog and synthesize them with Synopsys Design Compiler. The synthesis is performed at 0.5 GHz using the Nangate 45nm OpenCell Library to estimate area and power. Each MAC unit is sized to iteratively add 64 terms from a dot product.

4.2. Experiment Results

Main Results. As shown in Table 1, BlockDialect consistently outperforms MXFP4 across all models within the *linear* scope, even at a lower effective bitwidth. For instance, with a block size of 64 (lower effective bitwidth than MXFP4’s block size of 32), BlockDialect achieves a 0.95-point lower perplexity and 2.82% improvement in zero-shot accuracy on the LLaMA3 model. Additionally, BlockDialect surpasses both LLM-FP4 and Quarot, with 41.41/0.72-point lower perplexity, and 29.59% / 4.59% accuracy improvement, respectively. Compared to full-precision results, BlockDialect with a block size of 32 exhibits marginal accuracy drops of 2.22%, 1.20%, and 1.46% on the LLaMA3, LLaMA2, and Mistral models, respectively.

One key achievements of BlockDialect is its ability to quantize the operands of full-path matrix multiplications (*all*), while maintaining robust performance. While MXFP4 suffers a significant $\sim 17.29\%$ accuracy drop even with a 16-block size, BlockDialect with a 32-block size shows resilience, with only 5.89%, 3.31%, and 2.70% accuracy degradation compared to full precision on the LLaMA3, LLaMA2, and Mistral models, respectively. Notably, BlockDialect surpasses Quarot (W4A4KV4), which quantizes the linear layer, key, and value to 4-bit, demonstrating BlockDialect’s superiority. It is worth noting that the comparison with W4A4KV4 is conservative, as it retains query and attention score in high precision and performs high-precision

⁴<https://github.com/microsoft/microxcaling>

Table 1. Perplexity on Wikitext2 and average zero-shot accuracy across seven common-sense reasoning tasks: LAMBADA (LA), WinoGrande (WG), BoolQ (BQ), PIQA (PQ), ARC-easy (A-e), ARC-challenge (A-c), and HellaSwag (HS). *dn*: down_proj, *Q*: query, *K*: key, *V*: value. †: Quarot keeps query and attention scores in FP16 and performs the associated operations in FP16.

Scope	Method	Block size (exception)	LLaMA3-8B			LLaMA2-7B			Mistral-7B			
			Eff. bit	Wiki↓	AVG.↑	Eff. bit	Wiki↓	AVG.↑	Eff. bit	Wiki↓	AVG.↑	
-	FP16	-	16	6.14	74.46	16	5.47	70.94	16	5.32	74.92	
Linear ($A*W$)	LLM-FP4	A:tensor, W:ch.	4	48.71	41.92	4	15.61	58.15	4	17.47	58.47	
	Quarot (W4A4)	A:token, W:ch.	4	8.02	66.92	4	6.04	68.00	4	5.74	72.49	
	MXFP4	16	4.31	8.19	68.72	4.31	7.07	68.86	4.31	6.49	70.62	
		32	4.16	8.25	68.69	4.16	7.04	65.94	4.16	6.42	70.24	
	BlockDialect (w/ DialectFP4)	32	4.28	7.05	72.24	4.28	5.84	69.74	4.28	5.65	73.46	
		64	W:4.25	7.12	72.69	W:4.23	5.88	69.51	W:4.25	5.68	73.30	
	64	A:4.30	4.14	7.30	71.51	A:4.27	4.14	5.96	68.95	4.14	5.75	72.76
All ($A*W, A*A$)	Quarot (W4A4KV4)	A:token, W:ch. (K, V:128)	W,K,V:4†	8.17	66.01	W,K,V:4	6.10	67.50	W,K,V:4	5.80	71.72	
	MXFP4	16	4.31	18.84	57.17	4.31	11.22	60.73	4.31	9.27	66.32	
		32	4.16	16.69	58.89	4.16	11.14	59.76	4.16	8.98	65.07	
	BlockDialect (w/ DialectFP4)	32	4.28	7.87	68.57	4.28	6.33	67.63	4.28	5.87	72.22	
		64	W:4.25	7.77	69.00	W:4.23	6.35	68.29	W:4.25	5.90	71.66	
		64	A:4.21	8.55	66.60	A:4.21	6.63	67.09	A:4.21	6.07	70.17	
	64	4.14	8.55	66.60	4.14	6.63	67.09	4.14	6.07	70.17		

Table 2. Comparison of dialect selection methods.

Scope	Method	LLaMA3-8B		LLaMA2-7B		Mistral-7B	
		Wiki↓	0-shot↑	Wiki↓	0-shot↑	Wiki↓	0-shot↑
Linear	MSE	7.01	72.85	5.83	69.66	5.64	73.80
	Ours	7.05	72.24	5.84	69.74	5.65	73.46
All	MSE	7.72	69.19	6.25	68.37	5.85	72.10
	Ours	7.87	68.57	6.33	67.63	5.87	72.22

activation-activation multiplicaitons.

Finally, BlockDialect’s performance further improves with smaller block sizes in quantization-sensitive sublayers, as detailed in the following block size ablation study. This leads to accuracy drops of only 1.77% in the LLaMA3 linear scope, with 5.46% and 2.65% in the all scope for the LLaMA3 and LLaMA2 models, respectively, compared to full precision. Furthermore, BlockDialect outperforms MXFP4 by 11.83%, 7.56% while using fewer bits per data for these models.

Comparison of Dialect Selection: Exact MSE vs. Two-Stage Approach. We proposed an efficient two-stage approach to eliminate the need for real-time MSE calculation for activation quantization. Table 2 compares our method with the exact MSE-based approach, where both weight and activation dialects are selected based on MSE. Despite the absence of MSE computations, our approach in linear scope results in only a minor perplexity increase (~0.04) and a slight accuracy drop (~0.61%) across models, even when evaluated on the all scope (~0.15, ~0.74%), highlighting its effectiveness. This marginal performance gap also stems from the limitations of the exact MSE method, which over-

Table 3. Impact of block size: *dn*: down_proj *o*: output_proj, *q*: q_proj, *k*: k_proj, *v*: v_proj, *Q*: query, *K*: key.

Scope	Block size (exception)	LLaMA3-8B		LLaMA2-7B		Mistral-7B	
		Wiki↓	0-shot↑	Wiki↓	0-shot↑	Wiki↓	0-shot↑
Linear	16	6.82	72.98	5.76	69.91	5.55	73.39
	32	7.05	72.24	5.84	69.74	5.65	73.46
	64	7.30	71.51	5.96	68.95	5.75	72.76
	64 (<i>dn</i> :16)	7.12	72.69	5.88	69.51	5.68	73.30
	64 (<i>o</i> :16)	7.24	71.68	5.94	69.60	5.73	72.64
	64 (<i>q,k,v</i> :16)	7.19	71.66	5.91	69.28	5.68	73.30
All	16	7.32	70.64	5.76	69.91	5.71	72.54
	32	7.87	68.57	6.33	67.63	5.87	72.22
	64	8.55	66.60	6.63	67.09	6.07	70.17
	64	7.77	69.00	6.35	68.29	5.90	71.66
	(<i>dn,Q,K</i> :16)	7.77	69.00	6.35	68.29	5.90	71.66

looks the magnitude of data elements. This oversight can lead to suboptimal quantization, with inaccuracies for large magnitude values while accurately quantizing smaller ones. By focusing on large magnitudes, our method achieves more efficient and balanced quantization.

Impact of Block Size. We explore the impact of block size in Table 3. Overall, smaller sizes improve performance by constraining outliers within smaller blocks and making it easier to represent all block data more effectively with dialects. However, this advantage comes with a higher effective bitwidth, making it a trade-off between performance and memory footprint.

We further investigate dynamic block size assignment by applying small blocks to specific projection layers to assess block size sensitivity across sublayers. As in Table 3, down

Table 4. Comparison of *all* scope across different numbers of dialects: For the 8-dialect case, two formatbook construction configurations are tested: prioritizing large magnitude distribution (*dist.*) and dynamic range (maximum magnitude) of the block (*range*).

Dialect #	LLaMA3-8B		LLaMA2-7B		Mistral-7B	
	Wiki↓	0-shot↑	Wiki↓	0-shot↑	Wiki↓	0-shot↑
8 (<i>dist.</i>)	8.29	67.96	6.51	66.75	6.01	71.88
8 (<i>range</i>)	8.20	68.06	6.45	67.51	5.94	71.42
16	7.87	68.57	6.33	67.63	5.87	72.22
24	8.84	67.57	6.97	67.30	6.05	71.69

projection has higher sensitivity, which aligns with the observation from prior works (Li et al., 2023; Ashkboos et al., 2023). Based on these findings, we obtain comparable or superior results with block size of 64 by applying smaller blocks only to sublayers prone to outliers (Hooper et al., 2024; Liu et al., 2024a), compared to a uniform block size of 32. In-depth profiling of each sublayer’s block size sensitivity could lead to further optimization, which we leave as a future direction.

Impact of Number of Dialects. Table 4 compares the performance across different numbers of dialects. Since eight dialects are insufficient to cover both maximum magnitudes and large magnitude distribution, we generate two formatbooks with different priorities. The results demonstrate the effectiveness of the 16-dialect formatbook, which can address both maximum magnitudes and large magnitude distribution compared to the 8-dialect formatbook. Interestingly, prioritizing maximum magnitude (*range*) results in better performance than prioritizing distribution (*dist.*) overall, aligning with our two-stage approach: select a pair of dialects based on dynamic range first, then choose the better one based on its distribution. However, larger formatbook (beyond 16 dialects) struggles to identify the optimal dialect accurately, leading to reduced performance.

Additional Exploratory Studies. To explore various aspects of BlockDialect, we further analyze the dialect selection ratio for each model (Appendix B), confirming that all dialects are meaningful, with no extremely dominant or meaningless dialects. We also evaluate its performance on the OPT-6.7B (Zhang et al., 2022) model (Appendix D), verifying the effectiveness of BlockDialect in LLMs with different architectures. Additionally, we investigate the impact of block shape (Appendix E) and examine the synergy with different activation quantization approaches (Appendix F).

Hardware Comparison. DialectFP4 is compatible with 5-bit integer arithmetic operations, enabling two implementations: 1) leveraging the general INT4 MAC with simple logic (e.g., shifter) to handle residual bits for 5-bit multiplication (*Ours-INT4*), and 2) designing optimized MACs with 4-bit unsigned integer multiplier and additional XOR

Table 5. Comparison of MAC units with different number formats (0.5GHz, 45nm process). *Ours-INT4* refers to the implementation that leverages the widely adopted INT4 MAC, with additional logic. Area and power are in μm^2 and μW , respectively.

Type	Multiplier		Accumulator		Total	
	Area	Power	Area	Power	Area	Power
INT4	62.51	20.59	138.59	80.16	207.48	104.18
INT5	101.88	34.35	171.04	106.80	275.04	142.18
INT8	301.91	162.93	244.72	162.79	554.34	331.17
FP4	71.55	30.04	171.04	96.92	246.85	129.44
FP6	158.54	73.88	223.17	139.80	381.71	213.68
Ours	63.31	16.02	184.87	118.91	248.18	134.92
Ours-INT4	120.76	41.58	168.11	103.09	299.52	149.22

gate for sign bit (*Ours*). Although the first option requires more power and area, it could be a practical option since many commercial accelerators already adopt INT4 MACs. The second option’s MAC design achieves area and power efficiency comparable to FP4 (Table 5), providing significantly higher efficiency compared to higher precision MACs. Specifically, it is 1.58x (1.54x) more power (area) efficient than FP6 MACs, which are required to achieve better accuracy levels using the MX format (Rouhani et al., 2023b), and 2.45x (2.23x) more power (area) efficient than INT8 MACs. These results highlight how BlockDialect effectively utilizes non-uniform quantization to better capture magnitude distributions while leveraging hardware-efficient low-precision integer MACs.

5. Conclusion

In this work, we introduce *BlockDialect*, a hardware-efficient post-training quantization technique that assigns an optimal number format to fine-grained blocks. This approach allows BlockDialect to capture nuanced data distributions often overlooked by existing methods, thereby significantly enhancing representation accuracy. Complementing this, we develop *DialectFP4*, a set of FP4 variants, which ensure compatibility with an energy- and area-efficient integer MAC unit. To make this feasible, we propose an efficient method for online DialectFP4 activation quantization. Our 4-bit quantization results on the LLaMA3-8B (LLaMA2-7B) model affirm the superiority of our method, showcasing 11.83% (7.56%) accuracy improvement over MXFP4 at lower effective bitwidth, with only a minimal 5.46% (2.65%) accuracy gap compared to full precision for *full-path* quantization. By shifting the focus to how each block should be optimally represented in hardware-efficient manner, rather than solely scaling values, BlockDialect sets a foundation for energy-efficient LLM inference. This work offers a transformative pathway for advancing AI accelerators while balancing computational efficiency and model performance.

References

- Alizadeh, K., Mirzadeh, I., Belenko, D., Khatamifard, K., Cho, M., Del Mundo, C. C., Rastegari, M., and Farajtabar, M. LLM in a flash: Efficient Large Language Model Inference with Limited Memory. *arXiv preprint arXiv:2312.11514*, 2023.
- Ashkboos, S., Markov, I., Frantar, E., Zhong, T., Wang, X., Ren, J., Hoefler, T., and Alistarh, D. Towards End-to-end 4-Bit Inference on Generative Large Language Models. *arXiv preprint arXiv:2310.09259*, 2023.
- Ashkboos, S., Mohtashami, A., Croci, M. L., Li, B., Cameron, P., Jaggi, M., Alistarh, D., Hoefler, T., and Hensman, J. QuaRot: Outlier-Free 4-Bit Inference in Rotated LLMs. *arXiv preprint arXiv:2404.00456*, 2024.
- Bisk, Y., Zellers, R., Gao, J., Choi, Y., et al. Piqa: Reasoning about physical commonsense in natural language. In *Proceedings of the AAAI conference on artificial intelligence*, volume 34, pp. 7432–7439, 2020.
- Cao, Y., Wen, M., Luo, Z., Ju, X., Huang, H., Shen, J., and Chen, H. ABS: Accumulation Bit-Width Scaling Method for Designing Low-Precision Tensor Core. *IEEE Transactions on Very Large Scale Integration (VLSI) Systems*, 2024.
- Chee, J., Cai, Y., Kuleshov, V., and De Sa, C. M. QuIP: 2-bit Quantization of Large Language Models with Guarantees. *Advances in Neural Information Processing Systems*, 36, 2024.
- Chowdhery, A., Narang, S., Devlin, J., Bosma, M., Mishra, G., Roberts, A., Barham, P., Chung, H. W., Sutton, C., Gehrmann, S., et al. PaLM: Scaling Language Modeling with Pathways. *Journal of Machine Learning Research*, 24(240):1–113, 2023.
- Clark, C., Lee, K., Chang, M.-W., Kwiakowski, T., Collins, M., and Toutanova, K. BoolQ: Exploring the Surprising Difficulty of Natural Yes/No Questions. *arXiv preprint arXiv:1905.10044*, 2019.
- Clark, P., Cowhey, I., Etzioni, O., Khot, T., Sabharwal, A., Schoenick, C., and Tafjord, O. Think you have Solved Question Answering? Try ARC, the AI2 Reasoning Challenge. *arXiv preprint arXiv:1803.05457*, 2018.
- Dai, S., Venkatesan, R., Ren, M., Zimmer, B., Dally, W., and Khailany, B. VS-Quant: Per-Vector Scaled Quantization for Accurate Low-Precision Neural Network Inference. *Proceedings of Machine Learning and Systems*, 3:873–884, 2021.
- Dettmers, T., Lewis, M., Belkada, Y., and Zettlemoyer, L. GPT3.int8(): 8-bit Matrix Multiplication for Transformers at Scale. *Advances in Neural Information Processing Systems*, 35:30318–30332, 2022.
- Dettmers, T., Svirschevski, R., Egiazarian, V., Kuznedev, D., Frantar, E., Ashkboos, S., Borzunov, A., Hoefler, T., and Alistarh, D. SpQR: A Sparse-Quantized Representation for Near-Lossless LLM Weight Compression. *arXiv preprint arXiv:2306.03078*, 2023.
- Dettmers, T., Pagnoni, A., Holtzman, A., and Zettlemoyer, L. QLoRA: Efficient Finetuning of Quantized LLMs. *Advances in Neural Information Processing Systems*, 36, 2024.
- Dotzel, J., Chen, Y., Kotb, B., Prasad, S., Wu, G., Li, S., Abdelfattah, M. S., and Zhang, Z. Learning from Students: Applying t-Distributions to Explore Accurate and Efficient Formats for LLMs. *arXiv preprint arXiv:2405.03103*, 2024.
- Dubey, A., Jauhri, A., Pandey, A., Kadian, A., Al-Dahle, A., Letman, A., Mathur, A., Schelten, A., Yang, A., Fan, A., et al. The Llama 3 Herd of Models. *arXiv preprint arXiv:2407.21783*, 2024.
- Egiazarian, V., Panferov, A., Kuznedev, D., Frantar, E., Babenko, A., and Alistarh, D. Extreme Compression of Large Language Models via Additive Quantization. *arXiv preprint arXiv:2401.06118*, 2024.
- Frantar, E., Ashkboos, S., Hoefler, T., and Alistarh, D. GPTQ: Accurate Post-Training Quantization for Generative Pre-Trained Transformers. *arXiv preprint arXiv:2210.17323*, 2022.
- Gao, L., Tow, J., Abbasi, B., Biderman, S., Black, S., DiPofi, A., Foster, C., Golding, L., Hsu, J., Le Noac’h, A., Li, H., McDonnell, K., Muennighoff, N., Ociepa, C., Phang, J., Reynolds, L., Schoelkopf, H., Skowron, A., Sutawika, L., Tang, E., Thite, A., Wang, B., Wang, K., and Zou, A. A framework for few-shot language model evaluation, 12 2023. URL <https://zenodo.org/records/10256836>.
- Gholami, A., Kim, S., Dong, Z., Yao, Z., Mahoney, M. W., and Keutzer, K. A Survey of Quantization Methods for Efficient Neural Network Inference. In *Low-Power Computer Vision*, pp. 291–326. Chapman and Hall/CRC, 2022.
- Gholami, A., Yao, Z., Kim, S., Hooper, C., Mahoney, M. W., and Keutzer, K. AI and Memory Wall. *IEEE Micro*, 2024.
- Hooper, C., Kim, S., Mohammadzadeh, H., Mahoney, M. W., Shao, Y. S., Keutzer, K., and Gholami, A. KVQuant: Towards 10 Million Context Length LLM

- Inference with KV Cache Quantization. *arXiv preprint arXiv:2401.18079*, 2024.
- Jiang, A. Q., Sablayrolles, A., Mensch, A., Bamford, C., Chaplot, D. S., Casas, D. d. l., Bressand, F., Lengyel, G., Lample, G., Saulnier, L., et al. Mistral 7B. *arXiv preprint arXiv:2310.06825*, 2023.
- Keles, F. D., Wijewardena, P. M., and Hegde, C. On the Computational Complexity of Self-Attention. In *International Conference on Algorithmic Learning Theory*, pp. 597–619. PMLR, 2023.
- Kim, S., Hooper, C., Gholami, A., Dong, Z., Li, X., Shen, S., Mahoney, M. W., and Keutzer, K. SqueezeLLM: Dense-and-Sparse Quantization. *arXiv preprint arXiv:2306.07629*, 2023.
- Kuzmin, A., Van Baalen, M., Ren, Y., Nagel, M., Peters, J., and Blankevoort, T. FP8 Quantization: The Power of the Exponent. *Advances in Neural Information Processing Systems*, 35:14651–14662, 2022.
- Li, Q., Zhang, Y., Li, L., Yao, P., Zhang, B., Chu, X., Sun, Y., Du, L., and Xie, Y. FPTQ: Fine-Frained Post-Training Quantization for Large Language Models. *arXiv preprint arXiv:2308.15987*, 2023.
- Lin, J., Tang, J., Tang, H., Yang, S., Chen, W.-M., Wang, W.-C., Xiao, G., Dang, X., Gan, C., and Han, S. AWQ: Activation-aware Weight Quantization for On-Device LLM Compression and Acceleration. *Proceedings of Machine Learning and Systems*, 6:87–100, 2024.
- Liu, S.-y., Liu, Z., Huang, X., Dong, P., and Cheng, K.-T. LLM-FP4: 4-bit Floating-Point Quantized Transformers. *arXiv preprint arXiv:2310.16836*, 2023a.
- Liu, Z., Oguz, B., Zhao, C., Chang, E., Stock, P., Mehdad, Y., Shi, Y., Krishnamoorthi, R., and Chandra, V. LLM-QAT: Data-Free Quantization Aware Training for Large Language Models. *arXiv preprint arXiv:2305.17888*, 2023b.
- Liu, Z., Yuan, J., Jin, H., Zhong, S., Xu, Z., Braverman, V., Chen, B., and Hu, X. KIVI: A Tuning-Free Asymmetric 2bit Quantization for KV Cache. *arXiv preprint arXiv:2402.02750*, 2024a.
- Liu, Z., Zhao, C., Fedorov, I., Soran, B., Choudhary, D., Krishnamoorthi, R., Chandra, V., Tian, Y., and Blankevoort, T. SpinQuant: LLM Quantization with Learned Rotations. *arXiv preprint arXiv:2405.16406*, 2024b.
- Merity, S., Xiong, C., Bradbury, J., and Socher, R. Pointer Sentinel Mixture Models. *arXiv preprint arXiv:1609.07843*, 2016.
- Nagel, M., Amjad, R. A., Van Baalen, M., Louizos, C., and Blankevoort, T. Up or Down? Adaptive Rounding for Post-Training Quantization. In *International Conference on Machine Learning*, pp. 7197–7206. PMLR, 2020.
- Paperno, D., Kruszewski, G., Lazaridou, A., Pham, Q. N., Bernardi, R., Pezzelle, S., Baroni, M., Boleda, G., and Fernández, R. The LAMBADA dataset: Word prediction requiring a broad discourse context. *arXiv preprint arXiv:1606.06031*, 2016.
- Rouhani, B. D., Zhao, R., Elango, V., Shafipour, R., Hall, M., Mesmakhosroshahi, M., More, A., Melnick, L., Golub, M., Varatkar, G., et al. With Shared Microexponents, A Little Shifting Goes a Long Way. In *Proceedings of the 50th Annual International Symposium on Computer Architecture*, pp. 1–13, 2023a.
- Rouhani, B. D., Zhao, R., More, A., Hall, M., Khodamoradi, A., Deng, S., Choudhary, D., Cornea, M., Dellinger, E., Denolf, K., et al. Microscaling Data Formats for Deep Learning. *arXiv preprint arXiv:2310.10537*, 2023b.
- Sakaguchi, K., Bras, R. L., Bhagavatula, C., and Choi, Y. WinoGrande: An Adversarial Winograd Schema Challenge at Scale. *Communications of the ACM*, 64(9):99–106, 2021.
- Sheng, Y., Zheng, L., Yuan, B., Li, Z., Ryabinin, M., Chen, B., Liang, P., Ré, C., Stoica, I., and Zhang, C. FlexGen: High-Throughput Generative Inference of Large Language Models with a Single GPU. In *International Conference on Machine Learning*, pp. 31094–31116. PMLR, 2023.
- Shyam, V., Pilault, J., Shepperd, E., Anthony, Q., and Millican, B. Tree Attention: Topology-aware Decoding for Long-Context Attention on GPU clusters. *arXiv preprint arXiv:2408.04093*, 2024.
- Touvron, H., Martin, L., Stone, K., Albert, P., Almahairi, A., Babaei, Y., Bashlykov, N., Batra, S., Bhargava, P., Bhosale, S., et al. Llama 2: Open Foundation and Fine-Tuned Chat Models. *arXiv preprint arXiv:2307.09288*, 2023.
- Tseng, A., Chee, J., Sun, Q., Kuleshov, V., and De Sa, C. QuIP#: Even Better LLM Quantization with Hadamard Incoherence and Lattice Codebooks. *arXiv preprint arXiv:2402.04396*, 2024.
- Wu, X., Yao, Z., and He, Y. ZeroQuant-FP: A Leap Forward in LLMs Post-Training W4A8 Quantization Using Floating-Point Formats. *arXiv preprint arXiv:2307.09782*, 2023.

- Xiao, G., Lin, J., Seznec, M., Wu, H., Demouth, J., and Han, S. SmoothQuant: Accurate and Efficient Post-Training Quantization for Large Language Models. In *International Conference on Machine Learning*, pp. 38087–38099. PMLR, 2023.
- Zellers, R., Holtzman, A., Bisk, Y., Farhadi, A., and Choi, Y. Hellaswag: Can a Machine Really Finish Your Sentence? *arXiv preprint arXiv:1905.07830*, 2019.
- Zhang, S., Roller, S., Goyal, N., Artetxe, M., Chen, M., Chen, S., Dewan, C., Diab, M., Li, X., Lin, X. V., et al. OPT: Open Pre-trained Transformer Language Models. *arXiv preprint arXiv:2205.01068*, 2022.
- Zhang, Y., Zhao, L., Cao, S., Zhang, S., Wang, W., Cao, T., Yang, F., Yang, M., Zhang, S., and Xu, N. Integer or Floating Point? New Outlooks for Low-Bit Quantization on Large Language Models. In *2024 IEEE International Conference on Multimedia and Expo (ICME)*, pp. 1–6. IEEE, 2024.
- Zhao, Y., Lin, C.-Y., Zhu, K., Ye, Z., Chen, L., Zheng, S., Ceze, L., Krishnamurthy, A., Chen, T., and Kasikci, B. ATOM: Low-Bit Quantization for Efficient and Accurate LLM Serving. *Proceedings of Machine Learning and Systems*, 6:196–209, 2024.

A. Block-Level Profiling Results

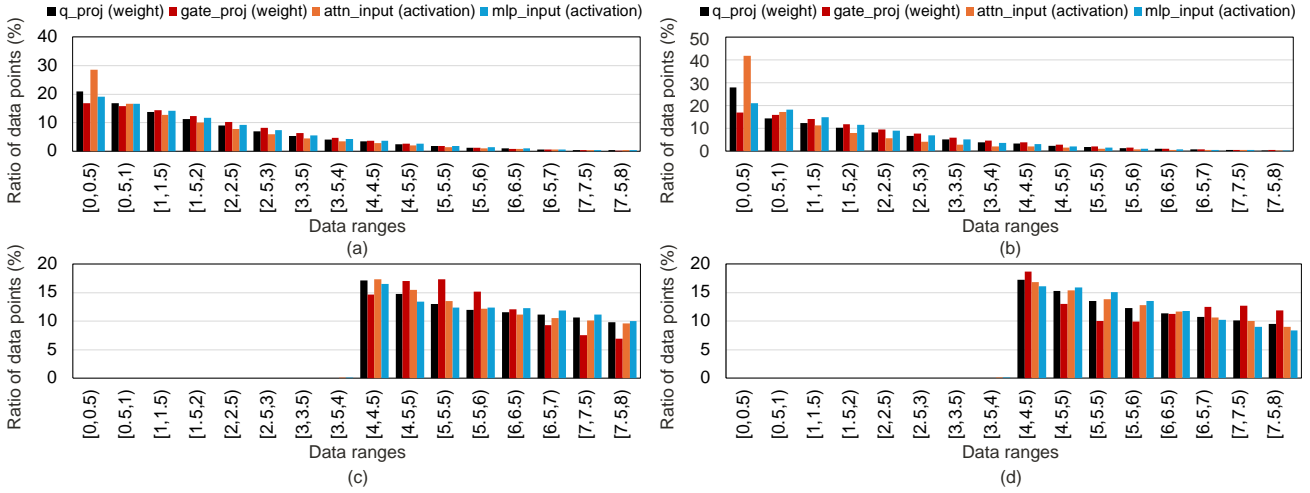


Figure 7. LLaMA-7B (a,c) and Mistral-7B (b,d) Block-level profiling results: (a), (b) matrix-wise accumulated magnitude distribution, (c), (d) block’s maximum magnitude distribution.

Figure 7 presents the block-level profiling results for the LLaMA2 and Mistral models. Each matrix is divided into blocks of size 32, with each block scaled by the shared exponent, $\lfloor \log_2(\text{block’s maximum magnitude}) \rfloor - 2$. Magnitude distribution histograms are then accumulated for each block. Figure 7 shows the average results for layers 0, 10, 20, and 30 of the LLaMA2 and Mistral models, showing a similar trend to LLaMA3 as discussed in Section 3.1.

B. Dialect Selection Ratio

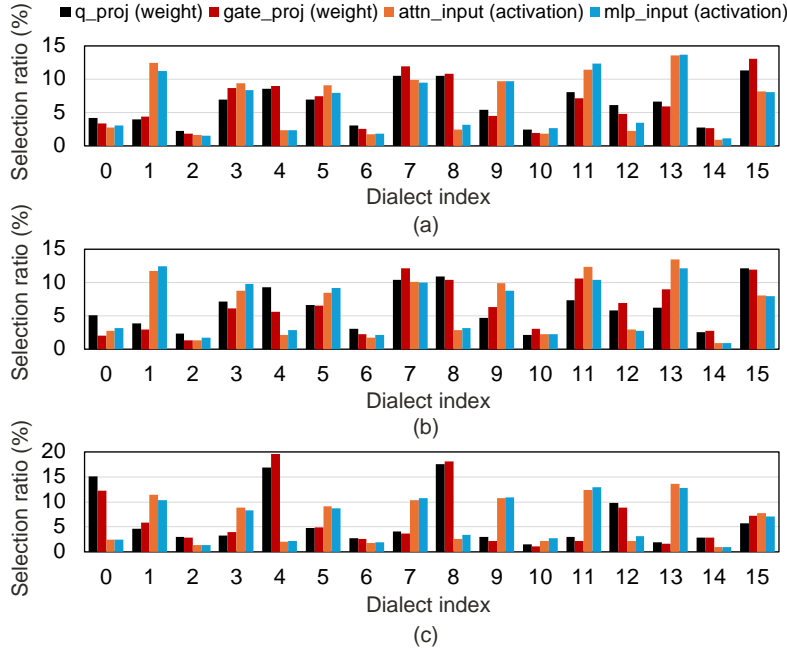


Figure 8. Selection ratio of each dialect for (a) LLaMA3-8B, (b) LLaMA2-7B, and (c) Mistral-7B. Experiments were conducted on Wikitext2 with a block size of 32. Each bar represents the average across layers 0, 10, 20, and 30.

Figure 8 illustrates the selection ratio of each dialect across three models. While the Mistral model shows a slightly higher concentration in selecting specific dialects, all dialects are effectively utilized, with no dialect being overwhelmingly dominant or insignificant. Interestingly, the weights of the Mistral model are more likely to select dialects with larger values (even-number dialects) compared to other models. Unlike weights, activations of all models tend to favor dialects skewed towards smaller values (odd-numbered dialects).

C. Quantization Dimension

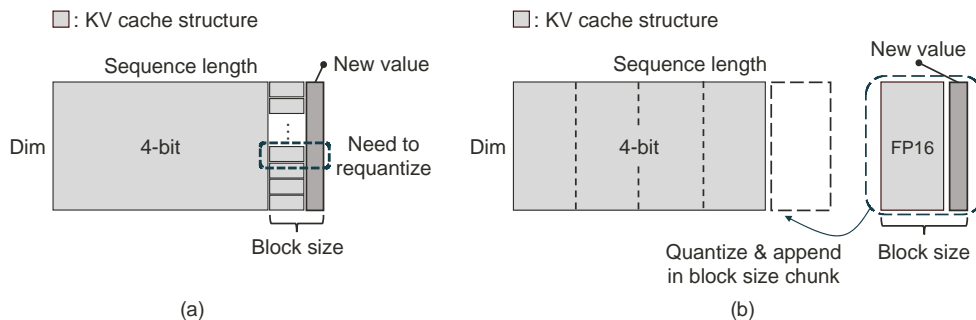


Figure 9. Proposed KV cache structure: (a) challenge of sub-channel-wise value quantization, (b) proposed cache structure.

BlockDialect quantizes matrices and vectors along their respective multiplication dimensions. For example, in activation-weight multiplication, activations are quantized at the sub-token level, while weights are quantized at the sub-channel level. Existing KV cache quantization approaches, such as per-token quantization (Sheng et al., 2023), per-channel key quantization with non-uniform representation (Hooper et al., 2024) or group-wise quantization (Ashkboos et al., 2024), primarily focus on compressing and reducing I/O costs during the *decode phase*. These approaches often dequantize data to FP16 before performing multiplications, which limits computational efficiency. In contrast, BlockDialect addresses the full computational path, achieving both memory savings and hardware-efficient computation without FP16 multiplications. Note that BlockDialect’s full-path low-precision matrix multiplication is significantly more efficient during the *prefill phase*.

To achieve this, BlockDialect employs sub-token-wise quantization for keys and sub-channel-wise quantization for values, aligning with the respective multiplication dimensions. However, this design introduces a challenge: repeated quantization overhead and numerical inconsistencies when updating the KV cache. Specifically, while sub-token-wise key quantization is straightforward, as new key vectors can be quantized before multiplication and appended to the KV cache, sub-channel-wise value quantization is more complex. When a new value vector is added, the values of each sub-channel must be requantized (Figure 9a). However, BlockDialect discards the FP16 value and directly dequantizes to 5-bit integers with a shared exponent to leverage integer arithmetic operations. As a result, requantizing from the 5-bit integer quantized form risks quantization errors when integrating new value vectors.

To address this, we can leverage *fine-grained* block structure with a default size of 32. Values are stored in 4-bit chunks of $block_size$ token count, with only the most recent chunk (size of $N \bmod block_size$) maintained in high precision. Instead of requantizing all blocks of the most recent chunk for every new value vector, once this chunk’s token count reaches the block size, then the chunk is stored in 4-bit form⁵ (Figure 9b). This strategy avoids excessive quantization and ensures accurate updates while keeping the small number of high-precision tokens (low portion relative to the total sequence length), resulting in minimal additional storage cost. Similar to Section 4.2, smaller block can be used for KV cache quantization, further reducing the overhead and enhancing model performance.

D. Experimental Results on a Different Architecture

We further evaluate BlockDialect on an LLM with a different architecture, OPT-6.7B (Zhang et al., 2022) in Table 6. With a 32-block size, BlockDialect achieves significant gains over MXFP4 (16-block size), showing 7.86 and 11.31 lower perplexity points, along with 9.70% and 10.54% zero-shot accuracy improvements in *linear* and *all* scopes, respectively. When using a

⁵Similar architecture to the residual cache in <https://huggingface.co/blog/kv-cache-quantization>, which targets to reduce repeated quantization and preserve accuracy for recent keys and values.

Table 6. Results on **OPT-6.7B** model. Perplexity on Wikitext2 and zero-shot accuracy across seven common-sense reasoning tasks: LAMBADA (LA), WinoGrande (WG), BoolQ (BQ), PIQA (PQ), ARC-easy (A-e), ARC-challenge (A-c), and HellaSwag (HS).

Scope	Method	Block size	Feature	Eff. bit	Wiki↓	LA↑	WG↑	BQ↑	PQ↑	A-e↑	A-c↑	HS↑	AVG.↑
-	FP16	-	Full precision	16	10.86	67.63	65.43	66.12	76.55	60.14	34.81	67.19	62.55
Linear	MXFP4	16	HW-supported scaling	4.31	19.17	49.78	52.41	50.06	69.31	47.39	28.92	56.64	50.64
		32		4.16	19.22	49.89	54.93	49.54	69.10	46.89	29.44	56.04	50.83
	BlockDialect (w/ DialectFP4)	16	1D block	4.56	11.26	66.89	64.48	62.57	76.55	58.71	34.90	65.20	61.33
		32		4.28	11.31	65.73	64.40	62.11	75.68	57.58	32.17	64.69	60.34
		64		4.14	11.73	63.21	61.33	63.43	74.81	58.12	33.02	63.16	59.58
	All	MXFP4	16	HW-supported scaling	4.31	22.94	45.06	53.28	48.23	68.39	45.45	28.24	53.98
32			4.16		22.12	44.25	50.51	45.93	63.49	44.15	29.27	53.81	47.34
BlockDialect (w/ DialectFP4)		16	1D block	4.56	11.45	64.93	63.61	60.80	75.19	58.71	33.19	64.70	60.16
		32		4.28	11.63	64.62	61.96	59.63	75.35	58.21	32.85	63.82	59.49
		64		4.14	12.14	59.32	60.06	60.37	74.16	57.28	32.34	62.84	58.05

Table 7. Impact of block shape: 2D block shapes of sizes 16, 32, and 64 have dimensions of (4,4), A(4,8) or W(8,4), and (8,8), respectively.

Scope	Block size (shape)	LLaMA3-8B		LLaMA2-7B		Mistral-7B	
		Wiki↓	0-shot↑	Wiki↓	0-shot↑	Wiki↓	0-shot↑
Linear	16 (1D)	6.82	72.98	5.76	69.91	5.55	73.39
	16 (2D)	6.87	73.15	5.81	69.54	5.57	73.93
	32 (1D)	7.05	72.24	5.84	69.74	5.65	73.46
	32 (2D)	7.09	71.97	5.92	69.09	5.65	73.15
	64 (1D)	7.30	71.51	5.96	68.95	5.75	72.76
	64 (2D)	7.33	71.60	6.06	69.24	5.79	71.99
All	16 (1D)	7.32	70.64	6.08	68.66	5.71	72.54
	16 (2D)	7.47	71.00	6.22	69.11	5.84	72.91
	32 (1D)	7.87	68.57	6.33	67.63	5.87	72.22
	32 (2D)	7.89	68.58	6.51	67.55	5.95	72.39
	64 (1D)	8.55	66.60	6.63	67.09	6.07	70.17
	64 (2D)	8.51	67.23	6.88	67.43	6.09	70.67

16-block size, BlockDialect is only 1.22% and 2.39% behind full precision in *linear* and *all* scopes, respectively.

E. Impact of Block Shape

So far, we have experimented exclusively with 1D linear-shaped blocks. However, 2D square-shaped blocks may prove advantageous, as they can better capture channel-wise activation variance compared to sub-token-wise linear-shaped blocks. We compare perplexity and zero-shot common-sense reasoning task accuracy between linear and square-shaped blocks in Table 7. While the 2D block shows slightly better accuracy for *all* scope, there is no clear superiority between 1D and 2D blocks in terms of accuracy. However, 2D block quantization generally results in higher perplexity. We infer that, due to the significant channel-wise variance of the key (Liu et al., 2024a), 2D block quantization for the key in *all* scope results in marginally better accuracy than sub-token-wise 1D block key quantization, while 2D block quantization for the linear layer has minimal impact with small block size.

It is important to note the lm-eval-harness framework processes multiple tokens in parallel, akin to the *prefill phase*. As a result, the reported numbers may not fully capture the impact of block shape during the *decode phase*. In the *decode phase*, operations typically involve GEMV or flat GEMM, which require zero padding for the square shape quantization. This results in an increased effective bitwidth for square-shaped blocks, as the scaling factor is calculated over fewer non-padding elements compared to the full block size. At the same time, it could be beneficial for accuracy, as the effective block size for

Table 8. Synergistic Effects of combining SmoothQuant with different LLMs.

Method	Wiki↓	0-shot↑
LLaMA3-8B w/o SmoothQuant	7.30	71.51
LLaMA3-8B w/ SmoothQuant	7.21	71.54
LLaMA2-7B w/o SmoothQuant	5.96	68.95
LLaMA2-7B w/ SmoothQuant	5.89	69.08
Mistral-7B w/o SmoothQuant	5.75	72.76
Mistral-7B w/ SmoothQuant	5.66	73.02
OPT-6.7B w/o SmoothQuant	11.73	59.58
OPT-6.7B w/ SmoothQuant	11.25	61.27

scaling becomes smaller for padded blocks.

F. Combination with Other Approach

To explore potential synergy with other approaches, we combine BlockDialect with SmoothQuant (Xiao et al., 2023), which shifts the challenge of activation quantization to the weights. We experiment with various migration strengths (α), controlling the aggressiveness of this shift with a granularity of 0.05, and select the most effective one with the lowest perplexity. For a block size of 64, applying SmoothQuant results in 0.09, 0.07, 0.09, and 0.48 points of perplexity improvement, along with 0.03%, 0.13%, 0.26%, and 1.69% accuracy gain in the LLaMA3-8B, LLaMA2-7B, Mistral-7B, and OPT-6.7B models, respectively. This demonstrates an overall improvement from the combination, though the gains are limited in some models.

We hypothesize that, despite the distinct perspectives of BlockDialect and SmoothQuant, they are not entirely orthogonal. Specifically, methods that *flatten* the distribution (like SmoothQuant or other techniques using a rotation matrix) may influence the performance of our approach, which focuses on selecting the best dialect for each distinct *fluctuating* distribution. We believe an optimal balance exists between both approaches. For example, extreme-magnitude outliers could be handled by flattening them using SmoothQuant (or other methods), while moderate outliers could be addressed with BlockDialect. We leave this as an area for future investigation.

G. Effective Bitwidth Calculation

Effective bitwidth is defined as the average bitwidth required per data element, incorporating overhead from scaling factors and dialect identifiers. Based on FP16 for full precision, a 5-bit shared exponent is used per block for the MX format, contributing an overhead of $5/block_size$. In BlockDialect, an additional 4-bit overhead per block is required to encode the optimal dialect index (with 16 dialects in the formatbook by default), resulting in a total overhead of $9/block_size$.

For mixed block sizes, we individually calculate the effective bitwidth for weights and activations to offer a clearer and more precise understanding. The weight calculation is straightforward, but activation quantization considers two possible approaches due to shared activations across multiple projections: 1) weighted summation for shared activations, and 2) counting shared activations only once. The first approach captures computational overhead more accurately, while the second is suited for memory-centric analyses. Since activations are more relevant to computational context, we adopt the first approach. Additionally, for activation-activation multiplications in the attention mechanism, the sequence length affects the effective bitwidth. For example, the attention score involves two dimensions of sequence length, whereas other operands use only one. We base our calculations on a sequence length of 2048. Finally, for per-token or per-channel quantization with software supported high-precision scaling factor, we omit overhead calculations as they are negligible.

H. Full Results

The following tables present the complete experimental results for three models: LLaMA3-8B, LLaMA-7B, and Mistral-7B, respectively.

Table 9. Full results on **LLaMA3-8B** model. Perplexity on Wikitext2 and zero-shot accuracy across seven common-sense reasoning tasks: LAMBADA (LA), WinoGrande (WG), BoolQ (BQ), PIQA (PQ), ARC-easy (A-e), ARC-challenge (A-c), and HellaSwag (HS). dn : down_proj o : output_proj, q : q_proj, k : k_proj, v : v_proj, Q : query, K : key, and V : value. 2D block shapes of sizes 16, 32, and 64 have dimensions of (4,4), A(4,8) or W(8,4), and (8,8), respectively. †: Quarot keeps query and attention scores in FP16 and performs the associated operations in FP16.

Scope	Method	Block size	Feature	Eff. bit	Wiki↓	LA↑	WG↑	BQ↑	PQ↑	A-e↑	A-c↑	HS↑	AVG.↑	
-	FP16	-	Full precision	16	6.14	76.05	72.77	81.38	80.79	77.74	53.33	79.18	74.46	
Linear	LLM-FP4	A:tensor, W:ch.	Mixed format	4	48.71	22.45	52.88	60.31	58.22	39.31	22.10	38.14	41.92	
	Quarot (W4A4)	A:token, W:ch.	Rotation matrix	4	8.02	67.65	67.09	72.84	75.73	70.45	41.89	72.78	66.92	
	MXFP4		16	HW-supported scaling	4.31	8.19	69.49	69.46	72.51	78.56	71.55	45.99	73.46	68.72
			32		4.16	8.25	68.58	68.82	72.69	77.69	72.73	46.59	73.72	68.69
			64		4.08	8.34	67.28	68.67	72.32	76.77	69.78	46.25	73.22	67.76
	BlockDialect (w/ DialectFP4)	16		1D block	4.56	6.82	75.10	71.74	80.76	80.41	74.75	50.77	77.35	72.98
				2D block	4.56	6.87	74.75	71.67	80.92	79.71	77.10	50.34	77.56	73.15
		32		1D block	4.28	7.05	73.96	72.14	78.62	78.40	74.92	50.94	76.69	72.24
				2D block	4.28	7.09	73.80	70.96	80.15	79.33	74.83	48.12	76.57	71.97
				Exact MSE	4.28	7.01	74.09	71.03	79.57	79.92	76.60	51.71	77.02	72.85
		64		1D block	4.14	7.30	72.54	70.80	77.89	78.35	75.17	49.91	75.90	71.51
				2D block	4.14	7.33	74.11	71.43	77.98	78.45	74.75	48.38	76.11	71.60
				w/ SmoothQuant	4.14	7.21	73.04	70.24	78.17	78.89	75.13	49.57	75.74	71.54
				dn block size:16	W:4.25 A:4.30	7.12	73.22	71.59	78.81	79.33	77.53	51.45	76.91	72.69
				o block size:16	W:4.17 A:4.19	7.24	72.97	68.98	78.35	78.29	76.05	50.68	76.47	71.68
		q,k,v block size:16	W:4.19 A:4.27	7.19	73.37	70.48	77.19	79.11	75.97	49.23	76.24	71.66		
All	Quarot (W4A4KV4)	A:token, W:ch.	K,V block size:128	W,K,V:4†	8.17	67.15	67.17	71.41	75.08	67.55	40.78	72.96	66.01	
	MXFP4	16	HW-supported scaling	4.31	18.84	52.51	59.91	64.22	71.00	59.47	34.98	58.07	57.17	
		32		4.16	16.69	58.78	61.48	64.62	71.44	59.34	35.41	61.14	58.89	
	BlockDialect (w/ DialectFP4)	16		1D block	4.56	7.32	73.24	69.69	77.71	77.69	73.11	47.01	76.06	70.64
				2D block	4.56	7.47	73.36	70.40	77.19	77.53	75.00	47.44	76.08	71.00
		32		1D block	4.28	7.87	71.76	66.54	74.89	76.33	71.25	44.62	74.62	68.57
				2D block	4.28	7.89	72.04	67.01	77.13	75.68	69.23	44.03	74.96	68.58
				Exact MSE	4.28	7.72	73.03	67.17	76.27	75.68	71.30	45.99	74.91	69.19
				8-dialect (dist.)	4.25	8.29	70.97	66.85	74.86	75.73	69.87	44.37	73.04	67.96
				8-dialect (range)	4.25	8.20	70.10	66.22	75.47	75.14	70.37	44.88	74.23	68.06
				24-dialect	4.31	8.84	70.75	66.46	74.10	75.19	68.39	44.88	73.21	67.57
		64		1D block	4.14	8.55	68.02	63.54	74.13	74.92	69.32	44.54	71.70	66.60
				2D block	4.14	8.51	70.74	64.96	75.14	74.37	68.39	43.52	73.46	67.23
dn,Q,K block size:16	W:4.25 A:4.21			7.77	71.08	66.38	77.37	75.24	71.63	47.18	74.12	69.00		

Table 10. Full results on **LLaMA2-7B** model. Perplexity on Wikitext2 and zero-shot accuracy across seven common-sense reasoning tasks: LAMBADA (LA), WinoGrande (WG), BoolQ (BQ), PIQA (PQ), ARC-easy (A-e), ARC-challenge (A-c), and HellaSwag (HS). dn : down_proj o : output_proj, q : q_proj, k : k_proj, v : v_proj, Q : query, K : key, and V : value. 2D block shapes of sizes 16, 32, and 64 have dimensions of (4,4), A(4,8) or W(8,4), and (8,8), respectively. †: Quarot keeps query and attention scores in FP16 and performs the associated operations in FP16.

Scope	Method	Block size	Feature	Eff. bit	Wiki↓	LA↑	WG↑	BQ↑	PQ↑	A-e↑	A-c↑	HS↑	AVG.↑	
-	FP16	-	Full precision	16	5.47	73.88	69.06	77.77	79.05	74.58	46.25	76.00	70.94	
Linear	LLM-FP4	A:tensor, W:ch.	Mixed format	4	15.61	57.97	61.80	66.45	69.48	57.07	32.76	61.55	58.15	
	Quarot (W4A4)	A:token, W:ch.	Rotation matrix	4	6.04	71.01	66.06	75.11	77.80	69.91	43.00	73.09	68.00	
	MXFP4		16	HW-supported scaling	4.31	7.07	69.84	68.11	72.14	77.31	68.35	41.38	70.86	66.86
			32		4.16	7.04	69.73	65.51	70.89	76.61	67.59	40.36	70.91	65.94
			64		4.08	7.05	70.58	65.11	71.25	76.50	68.35	40.70	70.81	66.19
	BlockDialect (w/ DialectFP4)	16		1D block	4.56	5.76	73.92	68.67	76.54	77.64	73.74	44.03	74.82	69.91
				2D block	4.56	5.81	73.49	66.61	76.61	78.56	72.90	43.94	74.66	69.54
		32		1D block	4.28	5.84	73.70	69.46	76.02	78.13	72.81	43.60	74.47	69.74
				2D block	4.28	5.92	72.27	66.30	76.85	77.80	72.73	43.43	74.24	69.09
				Exact MSE	4.28	5.83	73.24	68.27	76.88	78.13	72.39	44.28	74.44	69.66
		64		1D block	4.14	5.96	72.83	67.32	76.64	77.31	72.31	42.41	73.81	68.95
				2D block	4.14	6.06	73.04	66.61	77.49	77.86	72.18	44.37	73.16	69.24
				w/ SmoothQuant	4.14	5.89	72.27	67.17	75.87	77.48	72.64	43.60	74.54	69.08
				dn block size:16	W:4.23 A:4.27	5.88	72.40	68.90	76.88	78.62	72.26	43.69	73.82	69.51
				o block size:16	W:4.18 A:4.19	5.94	73.82	68.51	76.27	77.64	72.69	44.37	73.88	69.60
	q,k,v block size:16	W:4.25 A:4.29	5.91	73.26	67.88	76.82	77.58	72.43	42.66	74.35	69.28			
All	Quarot (W4A4KV4)	A:token, W:ch.	K,V block size:128	$W,K,V:4^\dagger$	6.10	70.79	64.33	74.40	77.20	70.12	42.92	72.72	67.50	
	MXFP4	16	HW-supported scaling	4.31	11.22	61.03	61.17	65.96	74.37	61.83	35.84	64.91	60.73	
		32		4.16	11.14	60.06	60.06	65.44	73.01	59.39	35.58	64.77	59.76	
	BlockDialect (w/ DialectFP4)	16		1D block	4.56	6.08	72.23	64.72	76.61	76.82	71.38	44.45	74.44	68.66
				2D block	4.56	6.22	72.09	67.48	76.30	77.48	72.52	43.34	74.55	69.11
		32		1D block	4.28	6.33	70.62	64.48	74.37	75.41	70.88	44.03	73.63	67.63
				2D block	4.28	6.51	70.75	67.40	73.58	76.50	69.32	41.55	73.77	67.55
				Exact MSE	4.28	6.25	71.18	66.69	75.41	77.69	71.17	42.83	73.62	68.37
				8-dialect (dist.)	4.25	6.51	69.30	62.98	73.52	76.66	69.74	42.32	72.73	66.75
				8-dialect (range)	4.25	6.45	70.75	63.22	74.37	77.26	70.20	43.34	73.41	67.51
		24-dialect	4.31	6.97	69.84	66.38	72.84	75.73	71.00	42.58	72.74	67.30		
		64		1D block	4.14	6.63	70.25	65.11	73.18	75.41	69.99	43.17	72.50	67.09
				2D block	4.14	6.88	70.66	65.04	73.52	76.66	69.57	43.52	73.03	67.43
	dn,Q,K block size:16			W:4.23 A:4.21	6.35	70.83	67.40	75.38	75.90	71.00	44.28	73.27	68.29	

Table 11. Full results on **Mistral-7B-v0.3** model. Perplexity on Wikitext2 and zero-shot accuracy across seven common-sense reasoning tasks: LAMBADA (LA), WinoGrande (WG), BoolQ (BQ), PIQA (PQ), ARC-easy (A-e), ARC-challenge (A-c), and HellaSwag (HS). dn : down_proj o : output_proj, q : q_proj, k : k_proj, v : v_proj, Q : query, K : key, and V : value. 2D block shapes of sizes 16, 32, and 64 have dimensions of (4,4), A(4,8) or W(8,4), and (8,8), respectively. †: Quarot keeps query and attention scores in FP16 and performs the associated operations in FP16.

Scope	Method	Block size	Feature	Eff. bit	Wiki↓	LA↑	WG↑	BQ↑	PQ↑	A-e↑	A-c↑	HS↑	AVG.↑	
-	FP16	-	-	16	5.32	75.32	73.88	82.11	82.26	78.24	52.22	80.42	74.92	
Linear	LLM-FP4	A:tensor, W:ch.	Mixed format	4	17.47	56.92	56.27	69.24	69.64	58.42	36.26	62.55	58.47	
	Quarot (W4A4)	A:token, W:ch.	Rotation matrix	4	5.74	72.75	70.24	78.87	80.58	77.44	49.57	77.99	72.49	
	MXFP4		16	HW-supported scaling	4.31	6.49	71.63	69.14	75.66	79.43	75.00	47.35	76.10	70.62
			32		4.16	6.42	71.88	67.25	74.86	79.65	74.33	47.61	76.08	70.24
			64		4.08	6.46	70.77	68.19	73.52	79.16	73.15	48.55	75.78	69.87
	BlockDialect (w/ DialectFP4)	16		1D block	4.56	5.55	73.80	70.56	80.43	81.45	77.36	50.60	79.54	73.39
				2D block	4.56	5.57	73.37	72.06	81.59	81.50	77.27	52.30	79.42	73.93
		32		1D block	4.28	5.65	73.45	71.11	81.13	81.83	77.31	50.17	79.20	73.46
				2D block	4.28	5.65	73.41	70.64	80.00	80.90	77.65	50.43	79.00	73.15
				Exact MSE	4.28	5.64	74.40	71.35	81.38	80.85	77.99	51.28	79.38	73.80
		64		1D block	4.14	5.75	73.08	69.85	79.63	80.69	77.19	49.83	79.04	72.76
				2D block	4.14	5.79	71.43	66.77	79.85	79.87	76.98	51.02	78.00	71.99
				w/ SmoothQuant	4.14	5.66	73.06	71.59	80.98	80.09	77.06	49.49	78.84	73.02
				dn block size:16	W:4.25 A:4.30	5.68	73.20	70.17	80.28	81.34	77.74	51.02	79.37	73.30
				o block size:16	W:4.17 A:4.19	5.73	72.79	69.69	78.38	80.52	77.40	50.43	79.27	72.64
			q,k,v block size:16	W:4.19 A:4.27	5.68	73.36	72.14	79.51	80.69	77.95	50.34	79.11	73.30	
All	Quarot (W4A4KV4)	A:token, W:ch.	K,V block size:128	$W,K,V:4^\dagger$	5.80	73.10	68.35	79.30	79.16	76.94	47.35	77.81	71.72	
	MXFP4	16	HW-supported scaling	4.31	9.27	65.46	65.90	71.50	76.82	70.33	42.32	71.88	66.32	
		32		4.16	8.98	64.68	61.88	70.46	76.77	69.15	41.04	71.49	65.07	
	BlockDialect (w/ DialectFP4)	16		1D block	4.56	5.71	72.56	69.93	79.54	80.20	76.56	49.91	79.06	72.54
				2D block	4.56	5.84	72.83	69.22	80.43	81.12	76.89	51.11	78.76	72.91
		32		1D block	4.28	5.87	71.73	69.93	80.49	80.47	75.97	48.55	78.38	72.22
				2D block	4.28	5.95	71.86	69.30	79.54	81.28	77.57	48.98	78.23	72.39
				Exact MSE	4.28	5.85	71.67	68.75	80.46	80.47	75.67	49.15	78.55	72.10
				8-dialect (dist.)	4.25	6.01	72.06	68.82	81.22	80.03	75.25	48.12	77.64	71.88
				8-dialect (range)	4.25	5.94	71.51	68.19	79.69	79.87	75.67	46.93	78.10	71.42
				24-dialect	4.31	6.05	71.01	69.38	79.14	80.58	75.04	48.89	77.82	71.69
		64		1D block	4.14	6.07	70.02	67.09	76.57	79.05	74.54	46.84	77.06	70.17
				2D block	4.14	6.09	70.25	64.64	79.66	79.27	75.46	48.55	76.83	70.67
dn,Q,K block size:16	W:4.25 A:4.21			5.90	71.24	70.01	78.07	79.33	75.55	49.49	77.92	71.66		